Research Article Vol. 59, No. 17 / 10 June 2020 / Applied Optics 5073

applied optics

Identification of microplastics in a large water volume by integrated holography and Raman spectroscopy

Tomoko Takahashi,[1,2,3,*] Zonghua Liu,[2] Thangavel Thevar,[4] Nicholas Burns,[4] Sumeet Mahajan,[3] Dhugal Lindsay,[1] John Watson,[4] and Blair Thornton[2,5]

[1]Advanced Science-Technology Research Program (ASTER), Japan Agency for Marine-Earth Science and Technology (JAMSTEC), 2-15 Natsushima-cho, Yokosuka, Kanagawa 2370061, Japan
[2]Institute of Industrial Science, The University of Tokyo, 4-6-1, Komaba, Meguro, Tokyo 1538505, Japan
[3]Department of Chemistry and the Institute for Life Sciences, University of Southampton, Southampton SO17 1BJ, UK
[4]School of Engineering, University of Aberdeen, AB24 3UE Scotland, UK
[5]Centre for In situ and Remote Intelligent Sensing, Faculty of Engineering and Physical Science, University of Southampton, Burgess Road, Southampton SO16 7QF, UK
*Corresponding author: takahas@jamstec.go.jp

Received 25 March 2020; revised 6 May 2020; accepted 7 May 2020; posted 7 May 2020 (Doc. ID 393643); published 2 June 2020

A noncontact method to identify sparsely distributed plastic pellets is proposed by integrating holography and Raman spectroscopy in this study. Polystyrene and poly(methyl methacrylate) resin pellets with a size of 3 mm located in a 20 cm water channel were illuminated using a collimated continuous wave laser beam with a diameter of 4 mm and wavelength of 785 nm. The same laser beam was used to take a holographic image and Raman spectrum of a pellet to identify the shape, size, and composition of material. Using the compact system, the morphological and chemical analysis of pellets in a large volume of water was performed. The reported method demonstrates the potential for noncontact continuous in situ monitoring of microplastics in water without collection and separation.

https://doi.org/10.1364/AO.393643

1. INTRODUCTION

Global awareness of plastic pollution in the marine environment has risen recently. In particular, the impact on ecology is a serious concern, with several reports of plastic waste being discovered in the guts of dead seabirds, turtles, and fish [1–4]. The density of plastic debris in the ocean has been selected as an indicator of the Sustainable Development Goals set by the United Nations for the year 2030 [5]. In particular, understanding the distribution of microplastics, whose size is defined as less than 5 mm [6], is becoming an urgent global issue. Microplastics get transported to all parts of the oceans, including the deep-sea trenches [7]. They are easily introduced into the food chain by being ingested by animals, and their impact on the organisms is the subject to multiple biological studies [8]. The sources of microplastics are either manufactured plastic components such as powder particles for scrubbers and resin pellets for plastic product manufacturing (primary sources), or small pieces made while plastic items decompose (secondary sources) [9]. To gauge the threat that microplastics pose, it is important to know their distribution on local and global scales, as well as any temporal changes. Typically, floating microplastic particles are collected together with other particles using a net towed by a ship, separated by their densities after dissolving organic matter, collected on a filter, and dried [6]. A plastic type of each particle on a filter is determined using spectroscopic methods, commonly Fourier-transform infrared (FT-IR) spectroscopy or Raman spectroscopy [10,11]. Since current techniques are dependent on sampling, the information is largely limited to surface distribution. While vertical profiles have been investigated using multiple nets [12], sample collection devices [13,14], and remotely operated vehicles [15], deployment of these systems are constrained by sea conditions and the number of samples is limited. In addition, recovering of all particles collected, including plankton and organic matters, is necessary, and separation and preparation of the samples are required for analysis. Data acquisition using this approach takes a long time and results in slow data feedback. While simulation-based research contributes to the understanding of the vertical transportation of microplastics [16], this research also requires ground truths with

measured values, and currently vertical profiles have been measured at limited locations. Temporal changes are also important to understand the interaction of organisms and microplastics [17], but are limited to long-term discrete information in small areas, such as seasonal differences. Since no practical in situ monitoring techniques currently exist, the temporal changes over short intervals during long-term measurements are not known.

Raman spectroscopy is a nondestructive molecular analytical method that has been widely used for identification of microplastics. It has been recently reported that microplastic particles flowing in water can be measured using Raman spectroscopy, while the water volume is limited, which demonstrates a large potential to chemically identify particle types in situ [18]. In general, optical methods, in particular laser spectroscopy, have advantages in in situ marine and deep-sea surveys since most of these methods are applicable to underwater targets [19–21], and Raman spectroscopy has been applied to the measurement of seawater and solids in the deep sea [22–25]. However, current in situ Raman spectroscopic analyzers are mostly used for bulk liquid analysis since solid measurement requires strict focusing to compensate for the inherently weak Raman scattering. In addition, measurement periods of several tens of seconds are often required. Therefore, it is not realistic to measure floating particles in a large volume of water for an application to deep-sea environments, where the total abundance of particles is several orders-of-magnitude lower than in shallow and coastal areas [26]. While in situ measurement of plastics collected using a filter is an option [27], the operation time depends on filtration capacity. A control system also is required to avoid filter blocking, which increases the system complexity and decreases the reliability for long-term deployments. Transmission Raman spectroscopy, often with a collimated or unfocused laser beam, is particularly effective in measurements of opaque, bulk solid targets [28,29] and has also demonstrated advantages in application fields such as measurements of pharmaceutical samples [30–32] and tissues [33]. While this technique so far only has been applied to a thin target in air, it also could be suitable to detect microplastic particles floating in the ocean without physical trapping on a membrane.

Optical holography is an imaging technique that can be applied to in situ monitoring of particles suspended in water. It is nondestructive, requires no sample preparation, and can make rapid measurement of particles in a relatively large water volume with high spatial (several tens of μm) and temporal (the order of μs) resolutions [34–36]. Compact in-line digital holographic devices have been widely used for in situ monitoring of marine distinctive particles such as plankton [37–40]. Holographic images can provide the size, shape, and position information of particles. It can also be used to automatically separate microplastics from organic particles using pattern recognition algorithms [41,42]. Yet, to determine plastic materials, chemical analysis is required. The setup configuration of holography, however, which consists of a single laser source and detector located at the other end of the beam, is the same as transmission Raman spectroscopy. These two methods could be combined into one setup to perform simultaneous or successive holography and Raman measurements, which would offer a compact hybrid system for microplastic identification.

In this study, we report a novel method for noncontact identification of microplastic resin pellets that integrates holography and Raman spectroscopy. Transmission Raman spectroscopy using a dual-purpose collimated beam that is also used for in-line holography was investigated to chemically identify a plastic particle suspended in water. Using a low electric power compact setup with a collimated laser beam for digital holography and Raman spectroscopy, target recognition and chemical identification are demonstrated for two different types of plastic resin pellets. In this approach, the rapid in-line holographic measurements can be used to detect and locate particles in a flow chamber. It can be used to trigger a flow trap that allows Raman measurements of the trapped particle to be performed so that its composition can be analyzed. This approach will enable selective Raman measurements of plastic or targeted particles by prescreening particles in a flow chamber using holographic images. This method is suitable for situations where other types of particles are mixed in a flow, such as in situ microplastic analysis in natural environments, particularly in the deep ocean where particles are sparsely distributed, and mostly no more than a single particle would be expected in a measurement volume at a time.

2. EXPERIMENTAL

A. Materials

Resin pellets of polystyrene (PS) and poly(methyl methacrylate) (PMMA) with a size of around 3 mm (Daikei Kagaku, Ltd.) were used in this study. Both pellets are transparent, similar in shape and size, and denser than the water, with the density of 1.04 g/cm^3 for PS and 1.18 g/cm^3 for PMMA. PS and PMMA are typically found in aquatic environments [43].

B. Setup

The experimental setup is shown in Fig. 1. Both holographic and Raman spectroscopic measurements were performed on a single pellet in a 20 cm channel. One end of a single-mode fiber (Thorlabs, P3-780AR-2) is connected to a single longitudinal mode continuous wave (CW) laser with a wavelength of 785 nm (Oxxius, LBX-785S-150-ISO-PPF); the other is attached to a collimator with a diameter of 4 mm (Thorlabs, F280APC-780), which is slightly larger than the pellet size, in a waterproof hull. The beam after the collimator passes through a 785 nm bandpass filter (Semrock, LL01-785-25) and sapphire window, and penetrates a channel filled with water, where a particle inside the channel was illuminated by the beam. After the second sapphire window, the laser beam is split in two at a 785 nm dichroic beam splitter (Semrock, Di03-R785-t1-25x36). Most of the beam is reflected by the beam splitter for holographic imaging, and the light with wavelengths longer than 785 nm is transmitted for Raman spectroscopy. The reflected light passed through two attenuation filters (OptoSigma, AND-25C-20, AND-25C-10) and was detected by a complementary metal-oxide semiconductor (CMOS) camera (JAI A/S, GO-5100-USB) connected to a laptop to monitor and record raw holographic images. Images were continuously taken with an exposure time of 7 μs, the minimum exposure time for the CMOS camera. The acquisition rate was 74 frames per second (fps). This camera

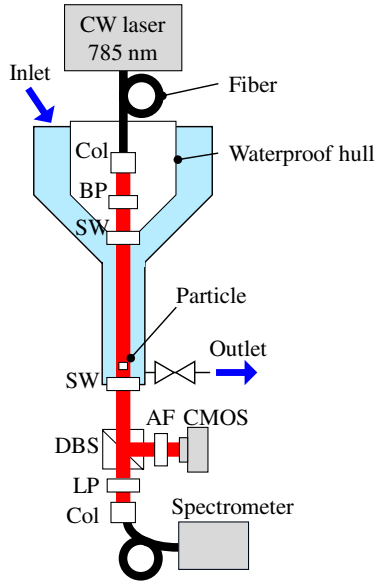

Fig. 1. Experimental setup: Col, collimator; BP, bandpass filter; SW, sapphire window; DBS, dichroic beamsplitter; AF, attenuation filter; and LP, longpass filter.

was chosen since it can take an image with such a short exposure time, which is important to avoid motion blur, especially when a CW laser is used for illumination. The transmitted light was collected using a collimator (Thorlabs, F110SMA-780) after a 785 nm longpass filter (Semrock, BLP01-785 R-25). It was transmitted through a multimode fiber with a core diameter of 600 μm (Thorlabs, M29L02) and the light was delivered to a spectrometer with a wavenumber range from 200 to 3100 cm^{-1} (Wasatch Photonics, WP-785-A-S-ER-25). The acquisition time was set to 30 s, since longer acquisition time did not increase the signal-to-noise ratio significantly. Background signals (i.e., taken using the same setup without a target) were subtracted from the spectra. Reference spectra were taken in air using a focusing probe (Wasatch Photonics, WP-785-RP) with an acquisition time of 5 s, which was experimentally found to be optimal for the condition in air, for each target.

C. Reconstruction of Holographic Images

The image reconstruction method used is explained in [44]. The angular spectrum method was used in this study [45]. Algorithms were implemented using Python 3.7.3. During algorithm development, images taken using a collimator with a diameter of 7.5 mm (Thorlabs, F810APC-780) were used to illuminate the entire area of the CMOS sensor. Figures 2(a) and 2(b) show examples of raw and reconstructed images, respectively, taken for a PS pellet located 20 cm from the detector. The laser power was set to 144 mW. It is clearly seen that the blurred edges of pellets in a raw image are sharpened in the reconstructed amplitude image. While three-dimensional analysis was not performed in this study since the light was not scattered sufficiently to record the surfaces of the cylindrical pellet, the width, length, and shape of the particle can be determined from the image.

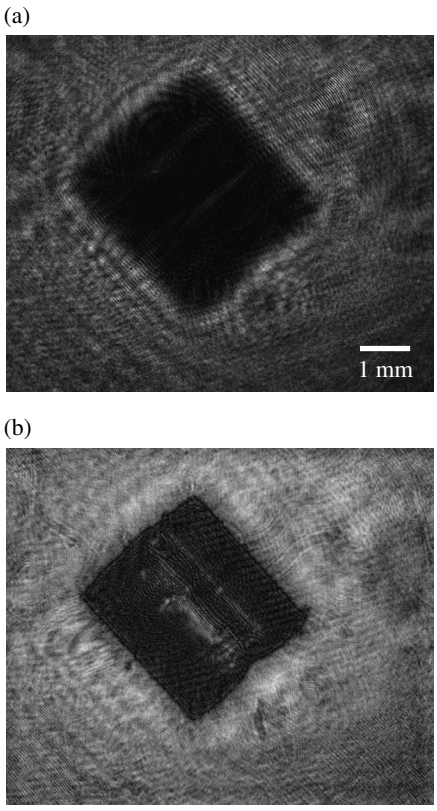

Fig. 2. (a) Raw and (b) reconstructed images of a PS pellet. The beam diameter for illumination was 7.5 mm.

3. RESULTS AND DISCUSSION

Figures 3(a) and 3(b) show the amplitude reconstruction of the digital holograms of PS and PMMA pellets, respectively, and Figs. 4(c) and 4(d) show Raman spectra of the same PS and PMMA pellets, respectively. The laser power for holography was set to 23 mW for PS and 18 mW for PMMA, which were found to be an optimal power for each target without saturation. The PMMA image in Fig. 3(b) has an artefact (stray diagonal line) that is most likely caused by a diffracted beam from one of the pellet edges. Regardless of the artefacts, we were able to extract the needed information from the hologram (i.e., the shape, dimensions, and relative position of the pellet). From Fig. 3, the width and length of pellets are calculated as 2.7 and 3.1 mm for PS, and 2.6 and 3.3 mm for PMMA, respectively, which is consistent with the actual size of the pellets. It can be said that the shape of pellets can be recognized using the beam with a diameter of 4 mm. Raman measurements were subsequently performed with the same beam diameter. While the laser power was increased to 75 mW, it is not problematic for the proposed measurement setup because the power of the laser can be changed through software without physical intervention once a particle has been confirmed. In Fig. 4, Raman spectra taken using the setup are shown in black, and reference Raman spectra taken for the same samples in air using a focused beam are shown in red. The maximum and minimum intensities of all the spectra are normalized to match each other. The Raman peaks of the targets are clearly seen in spectra taken for

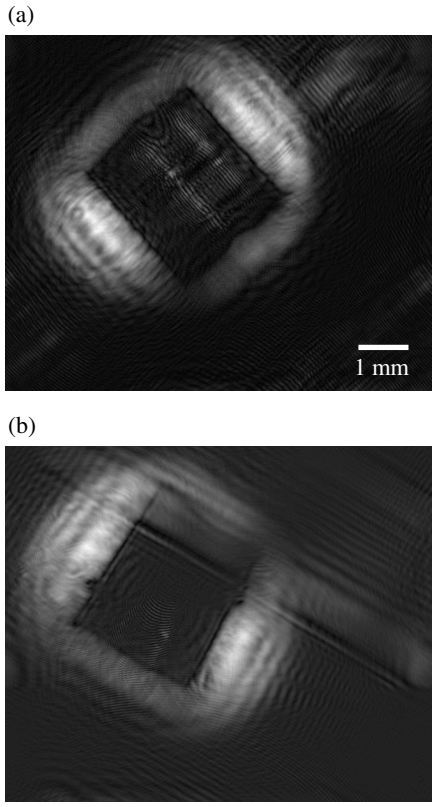

Fig. 3. Reconstructed holographic images of (a) PS and (b) PMMA pellets.

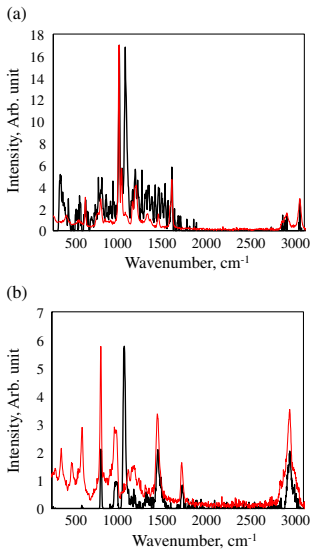

Fig. 4. Raman spectra of (a) PS and (b) PMMA pellets. Raman spectra taken using the setup are shown in black and reference Raman spectra taken for the same samples in air using a focused beam are shown in red.

underwater pellets. Table 1 summarizes the Raman peaks recognized. The listed peaks are those that are seen in the spectra taken in air and match references [46,47]. The PS peaks at 787, 996, 1027, 1151, 1191, 1596, and 3052 cm^{-1} [46] and PMMA peaks at 805, 969, 1237, 1445, 1721, and 2945 cm^{-1} [47] can be seen in the spectra taken in water. While a strong peak was observed at 1067 cm^{-1} in all the spectra taken in water, it does not match any peak of the targets. It is assumed to be a Raman peak of the Al-O bending mode of Al_2O_3 [48] used as a coating material to avoid corrosion of the measurement chamber. While the laser beam does not directly illuminate the chamber wall, a part of scattered beam on the target surface might be reflected at the wall, which causes Raman scattering of the wall material. Peaks at shorter wavelengths, especially for PMMA, were not observed in the signals taken in water, possibly because the peak heights were too low to be detected. It can be still said that the signal quality is high enough to identify the particle types and two pellets can be identified successfully using the proposed setup. Thus, the results confirm that both holography and Raman spectroscopy can be performed using a laser beam with a diameter of 4 mm. It should be noted that, although a beam diameter of 7.5 mm also was tested, distinguishable Raman signals could not be obtained. The power density of the beam diameter of 7.5 mm is 3.5 times less than the beam diameter of 4 mm, and the CCD used in this study does not have the sensitivity to collect the Raman scattering generated using a larger beam. A detector with a higher sensitivity will improve the detection limit and enable the proposed method to measure various sizes of microplastic particles using a large beam diameter. While two pellets were used in this study, the targets can be extended to other microplastic particle types, such as spheres and fibers. Although further studies are required to quantitatively analyze the threshold of power density and the minimum detectable size and types of particles, we have demonstrated for the first time that holography and Raman spectroscopy can

Table 1. Raman Peaks Seen in Spectra[a]

Raman Peaks in PS			
Ref. [46]	**In Air**	**1 mm**	**4 mm**
621	614	×	○
791	787	○	○
999	996	○	○
1031	1027	○	○
1165	1151	○	○
1200	1191	○	○
1449	1442	○	×
1606	1596	○	○
3056	3052	○	○
Raman Peaks in PMMA			
Ref. [47]	**In Air**	**1 mm**	**4 mm**
370	356	×	×
487	473	×	×
604	592	×	×
818	805	○	○
970	969	○	○
1234	1237	○	○
1456	1445	○	○
1736	1721	○	○
2957	2945	○	○

[a]The results are compared to references (Ref. [46] for PS and Ref. [47] for PMMA) and peaks seen in spectra taken in air with the focused system.

Table 2. Comparison of Specifications for In Situ Holographic and Raman Analyzers

Name	Method	Max. Power Consumption [W]	Measurement Volume [mL]	Acquisition Rate [fps]	Max. Speed of Particle Detection [mL/s]	Ref.
This paper	Raman + Holography	~30 (expected)	2.5	74	190	—
eHolocam	Holography	100	36.5	25	910	[40]
HoloSea (4-deep)	Holography	5	0.2	22	4.4	[49]
LISST-Holo2 (Sequoia Scientific, Inc.)	Holography	14	1.5	20	30	[50]
DORISS I & II	Raman	>50 (estimated)[a]	—	0.05–0.2	—	[22]

[a]The maximum power consumption of DORISS I and II was estimated by the components described in [22].

be performed using the same setup on suspended particles to obtain information about particle size, shape, and composition. Under the conditions with the diameter of 4 mm and a length of 20 cm, and with the acquisition rate of holography of 74 fps, the maximum speed of the flow is 190 mL/s for holographic particle detection. Table 2 compares the proposed method and existing in situ holography and Raman analyzers. Although the speed is moderate among conventional in situ oceanic holographic imaging devices, considering the power consumption, it can be said that the proposed method is efficient. It is because the proposed method only consists of a single low-power laser source, while a short-duration pulsed laser is used for typical in-line holographic measurements. The concept of the system is to perform continuous holographic monitoring to detect a particle, which can act as a trigger to pause the flow by closing a valve and initiating a Raman measurement. After the Raman measurement, the valve can be opened to resume the holographic monitoring to find the next particle. With this setup, the whole process can be performed automatically, which will be implemented in our future studies. Considering the ability to perform both holography and Raman spectroscopy in a systematic way to efficiently measure microplastic particles with such low power consumption, the proposed method has a great advantage for application to long-term platforms, such as autonomous underwater vehicles, ocean gliders, and Lagrangian floats for scalable ocean observation.

4. CONCLUSIONS

It has been demonstrated that holography and Raman spectroscopy can be performed using a single optical setup for microplastic pellets in water with a compact integrated setup. Plastic resin pellets of PS and PMMA with a size of 3 mm located in a 20 cm water channel can be detected from holographic images, and chemically identified with Raman spectroscopy using a CW laser beam with a diameter of 4 mm. This approach enables fast particle identification with both morphological and chemical information in a single, large volume channel.

Funding. Japan Science and Technology Agency SICORP (JPMJSC1705); Natural Environment Research Council (NE/R01227X/1); Kajima Foundation (Overseas research grant); Japan Society for the Promotion of Science (18H03810, 18K13934); Kurita Water and Environment Foundation (17B030).

Disclosures. The authors declare no conflicts of interest.

REFERENCES

1. C. J. Moore, "Synthetic polymers in the marine environment: a rapidly increasing, long-term threat," Environ. Res. **108**, 131–139 (2008).
2. M. Cole, P. Lindeque, C. Halsband, and T. S. Galloway, "Microplastics as contaminants in the marine environment: a review," Mar. Pollut. Bull. **62**, 2588–2597 (2011).
3. K. Tanaka and H. Takada, "Microplastic fragments and microbeads in digestive tracts of planktivorous fish from urban coastal waters," Sci. Rep. **6**, 34351 (2016).
4. D. Neves, P. Sobral, J. L. Ferreira, and T. Pereira, "Ingestion of microplastics by commercial fish off the Portuguese coast," Mar. Pollut. Bull. **101**, 119–126 (2015).
5. U. N. G. Assembly, "Work of the Statistical Commission Pertaining to the 2030 Agenda for Sustainable Development, "A/RES/71/313 (United Nations, 2017).
6. J. Masura, J. Baker, G. Foster, C. Arthur, and C. Herring, "Laboratory methods for the analysis of microplastics in the marine environment: Recommendations for quantifying synthetic particles in waters and sediments," Tech. Rep. NOS-OR&R-48, Carlie Herring, Ed. (National Oceanic and Atmospheric Administration Marine Debris Division, 2015).
7. T. Galloway and C. Lexis, "Marine microplastics," Curr. Biol. **27**, R445–R446 (2017).
8. S. L. Wright, R. C. Thompson, and T. S. Galloway, "The physical impacts of microplastics on marine organisms; a review," Environ. Pollut. **178**, 483–492 (2013).
9. V. Hidalgo-Ruz, L. Gutow, R. C. Thompson, and M. Thiel, "Microplastics in the marine environment: A review of the methods used for identification and quantification," Environ. Sci. Technol. **46**, 3060–3075 (2012).
10. R. C. Thompson, Y. Olsen, R. P. Mitchell, A. Davis, S. J. Rowland, A. W. G. John, D. McGonigle, and A. E. Russell, "Lost at sea: Where is all the plastic?" Science **304**, 838 (2004).
11. P. Ribeiro Claro, M. Nolasco, and C. Araújo, "Characterization of microplastics by Raman spectroscopy," Compreh. Anal. Chem. **75**, 119–151 (2016).
12. J. Reisser, B. Slat, K. Noble, K. Du Plessis, M. Epp, M. Proietti, J. De Sonneville, T. Becker, and C. Pattiaratchi, "The vertical distribution of buoyant plastics at sea: an observational study in the North Atlantic Gyre," Biogeosciences **12**, 1249–1256 (2015).
13. K. Enders, R. Lenz, C. A. Stedmon, and T. G. Nielsen, "Abundance, size and polymer composition of marine microplastics ≥10 μm in the Atlantic Ocean and their modelled vertical distribution," Mar. Pollut. Bull. **100**, 70–81 (2015).
14. K. K. La Daana, R. Officer, O. Lyashevska, R. C. Thompson, and I. O'Connor, "Microplastic abundance, distribution and composition

along a latitudinal gradient in the atlantic ocean," Mar. Pollut. Bull. **115**, 307–314 (2017).
15. C. A. Choy, B. H. Robison, T. O. Gagne, B. Erwin, E. Firl, R. U. Halden, J. A. Hamilton, K. Katija, S. E. Lisin, C. Rolsky, and K. S. Van Houtan, "The vertical distribution and biological transport of marine microplastics across the epipelagic and mesopelagic water column," Sci. Rep. **9**, 1–9 (2019).
16. T. Kukulka, G. Proskurowski, S. Morét-Ferguson, D. W. Meyer, and K. L. Law, "The effect of wind mixing on the vertical distribution of buoyant plastic debris," Geophys. Res. Lett. **39**, L07601 (2012).
17. A. R. A. Lima, M. Barletta, and M. F. Costa, "Seasonal distribution and interactions between plankton and microplastics in a tropical estuary," Estuarine, Coastal Shelf Sci. **165**, 213–225 (2015).
18. A. K. Kniggendorf, C. Wetzel, and B. Roth, "Microplastics detection in streaming tap water with Raman spectroscopy," Sensors **19**, 12–14 (2019).
19. C. Moore, A. Barnard, P. Fietzek, M. R. Lewis, H. M. Sosik, S. White, and O. Zielinski, "Optical tools for ocean monitoring and research," Ocean Sci. **5**, 661–684 (2009).
20. B. Thornton, T. Takahashi, T. Sato, T. Sakka, A. Tamura, A. Matsumoto, T. Nozaki, T. Ohki, and K. Ohki, "Development of a deep-sea laser-induced breakdown spectrometer for in situ multi-element chemical analysis," Deep Sea Res. Part I Oceanogr. Res. Pap. **95**, 20–36 (2015).
21. T. Takahashi, S. Yoshino, Y. Takaya, T. Nozaki, K. Ohki, T. Ohki, T. Sakka, and B. Thornton, "Quantitative in situ mapping of elements in deep-sea hydrothermal vents using laser-induced breakdown spectroscopy and multivariate analysis," Deep Sea Res. Part I Oceanogr. Res. Pap. **158**, 103232 (2020).
22. K. Hester, R. Dunk, P. Walz, E. Peltzer, E. Sloan, and P. Brewer, "Direct measurements of multi-component hydrates on the seafloor: pathways to growth," Fluid Phase Equilib. **261**, 396–406 (2007).
23. J. A. Breier, C. R. German, and S. N. White, "Mineral phase analysis of deep-sea hydrothermal particulates by a Raman spectroscopy expert algorithm: Toward autonomous in situ experimentation and exploration," Geochem., Geophys. Geosyst. **10**, 1–12 (2009).
24. X. Zhang, W. J. Kirkwood, P. M. Walz, E. T. Peltzer, and P. G. Brewer, "A review of advances in deep-ocean Raman spectroscopy," Appl. Spectrosc. **66**, 237–249 (2012).
25. X. Zhang, Z. Du, R. Zheng, Z. Luan, F. Qi, K. Cheng, B. Wang, W. Ye, X. Liu, C. Lian, C. Chen, J. Guo, Y. Li, and J. Yan, "Development of a new deep-sea hybrid Raman insertion probe and its application to the geochemistry of hydrothermal vent and cold seep fluid," Deep Sea Res. Part I Oceanogr. Res. Pap. **123**, 1–12 (2017).
26. D. J. Lindsay, A. Yamaguchi, M. M. Grossmann, J. Nishikawa, A. Sabates, V. Fuentes, M. Hall, K. Sunahara, and H. Yamamoto, "Vertical profiles of marine particulates: a step towards global scale comparisons using an Autonomous Visual Plankton Recorder," Bull. Plankton Soc. Jpn. **61**, 72–81 (2014).
27. E. C. Edson and M. R. Patterson, "MantaRay: a novel autonomous sampling instrument for in situ measurements of environmental microplastic particle concentrations," in *OCEANS 2015-MTS/IEEE Washington* (IEEE, 2015), pp. 1–6.
28. P. Matousek and A. W. Parker, "Bulk Raman analysis of pharmaceutical tablets," Appl. Spectrosc. **60**, 1353–1357 (2006).
29. K. Buckley and P. Matousek, "Recent advances in the application of transmission Raman spectroscopy to pharmaceutical analysis," J. Pharm. Biomed. Anal. **55**, 645–652 (2011).
30. P. Matousek and A. Parker, "Non-invasive probing of pharmaceutical capsules using transmission Raman spectroscopy," J. Raman Spectrosc. **38**, 563–567 (2007).
31. M. Foster, J. Storey, and M. Zentile, "Spatial-heterodyne spectrometer for transmission-Raman observations," Opt. Express **25**, 1598–1604 (2017).
32. K. A. Strange, K. C. Paul, and S. M. Angel, "Transmission Raman measurements using a spatial heterodyne Raman spectrometer (SHRS)," Appl. Spectrosc. **71**, 250–257 (2017).
33. N. Stone and P. Matousek, "Advanced transmission Raman spectroscopy: a promising tool for breast disease diagnosis," Cancer Res. **68**, 4424–4430 (2008).
34. J. Watson and P. W. Britton, "Preliminary results on underwater holography," Opt. Laser Technol. **15**, 215–216 (1983).
35. K. L. Carder, "A holographic micro-velocimeter for use in studying ocean particle dynamics," Proc. SPIE **160**, 63–66 (1978).
36. K. L. Carder, R. G. Steward, and P. R. Betzer, "In situ holographic measurements of the sizes and settling rates of oceanic particulates," J. Geophys. Res. **87**, 5681–5685 (1982).
37. J. Watson, S. Alexander, G. Craig, D. C. Hendry, P. R. Hobson, R. S. Lampitt, J. M. Marteau, H. Nareid, M. A. Player, K. Saw, and K. Tipping, "Simultaneous in-line and off-axis subsea holographic recording of plankton and other marine particles," Meas. Sci. Technol. **12** (2001).
38. J. Watson, S. Alexander, V. Chavidan, G. Craig, A. Diard, G. L. Foresti, S. Gentili, D. C. Hendry, P. R. Hobson, R. S. Lampitt, H. Nareid, J. J. Nebrensky, A. Pescetto, G. G. Pieroni, M. A. Player, K. Saw, S. Serpico, K. Tipping, and A. Trucco, "A holographic system for subsea recording and analysis of plankton and other marine particles (HOLOMAR)," in *Oceans Conference (IEEE)* (2003), pp. 830–837.
39. R. B. Owen and A. A. Zozulya, "In-line digital holographic sensor for monitoring and characterizing marine particulates," Opt. Eng. **39**, 2187 (2000).
40. H. Sun, P. W. Benzie, N. Burns, D. C. Hendry, M. A. Player, and J. Watson, "Underwater digital holography for studies of marine plankton," Philos. Trans. R. Soc. A **366**, 1789–1806 (2008).
41. F. Merola, P. Memmolo, V. Bianco, M. Paturzo, M. Mazzocchi, and P. Ferraro, "Searching and identifying microplastics in marine environment by digital holography," Europ. Phys. J. Plus **133**, 350 (2018).
42. V. Bianco, P. Memmolo, P. Carcagn, F. Merola, M. Paturzo, C. Distante, and P. Ferraro, "Microplastic identification via holographic imaging and machine learning," Adv. Intell. Syst. **2**, 1900153 (2020).
43. K. Duis and A. Coors, "Microplastics in the aquatic and terrestrial environment: sources (with a specific focus on personal care products), fate and effects," Environ. Sci. Euro. **28**, 2 (2016).
44. N. M. Burns and J. Watson, "Robust particle outline extraction and its application to digital in-line holograms of marine organisms," Opt. Eng. **53**, 112212 (2014).
45. N. Akhter, G. Min, J. W. Kim, and B. H. Lee, "A comparative study of reconstruction algorithms in digital holography," Optik **124**, 2955–2958 (2013).
46. J. R. Ferraro, J. S. Ziomek, and G. Mack, "Raman spectra of solids," Spectrochim. Acta **17**, 802–814 (1961).
47. H. A. Willis, V. J. Zichy, and P. J. Hendra, "The laser-Raman and infrared spectra of poly(methyl methacrylate)," Polymer **10**, 737–746 (1969).
48. N. J. Cherepy, T. H. Shen, A. P. Esposito, and T. M. Tillotson, "Characterization of an effective cleaning procedure for aluminum alloys: surface enhanced Raman spectroscopy and zeta potential analysis," J. Colloid Interface Sci. **282**, 80–86 (2005).
49. "HoloSea submersible microscope," 4Deep, http://4-deep.com/products/submersible-microscope/.
50. "LISST-Holo2,"Sequoia Scientific Inc., https://www.sequoiasci.com/product/lisst-holo/.